A Description of Sample Designs

In this paper, we consider three different families of sample design for our generalization gap analysis, namely random, blue noise and Poisson disk designs. Figure 4 illustrates the sample design along with their spectral/spatial properties for $d = 2$ and $N = 1000$. Note that, we show the 2D PSD here, though our analysis assumes isotropic distributions and hence uses radially averaged 1D-PSD.

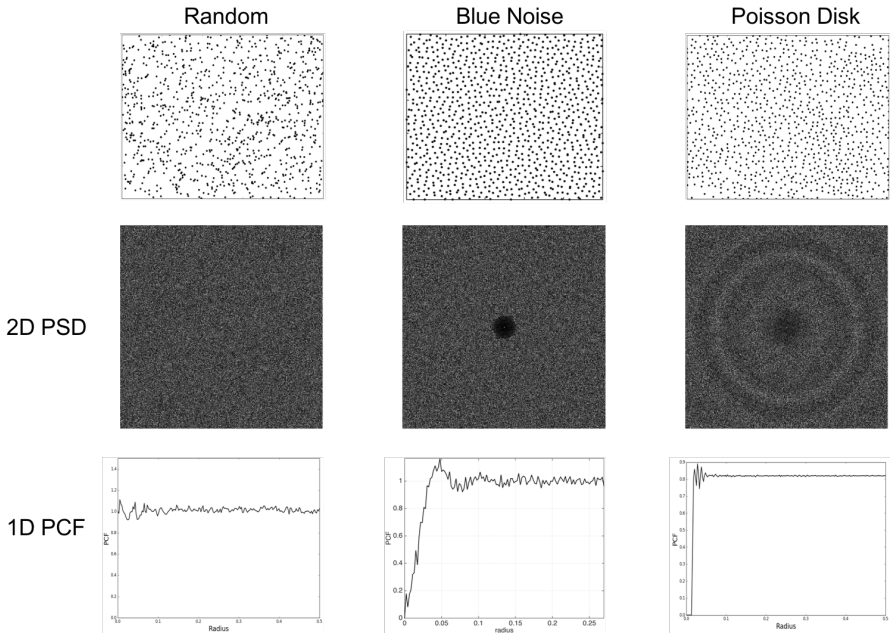

Figure 4: Sample design along with their spatial/spectral properties considered in our analysis.

B Proof of Theorem 1 from the main paper

We know that the PSD and PCF of a point distribution are related via the Fourier transform as follows:

$$\begin{aligned} P(\mathbf{k}) &= 1 + \rho F\left(G(\mathbf{r}) - 1\right) \\ &= 1 + N \int_{\mathbb{R}^d} \left(G(\mathbf{r}) - 1\right) \exp(-2\pi i \mathbf{k}.\mathbf{r}) d\mathbf{r} \end{aligned}$$

where $F(.)$ denotes the d-dimensional Fourier transform. Using symmetry of the Fourier transform, we have

$$G(\mathbf{r}) = 1 + \frac{1}{N} F\left(P(\mathbf{k}) - 1\right).$$

Next, we use polar coordinates with the z axis along $\mathbf{k}$, so that $\mathbf{k}.\mathbf{r} = \rho r \cos\theta$ where $\rho = |\mathbf{k}|$ and $r = |\mathbf{r}|$. For radially symmetric PCF, we have $G(\mathbf{r}) = G(r)$ and the above relationship can be rewritten as

$$\begin{aligned} G(r) &= 1 + \frac{1}{N} \int_0^\infty \int_0^\pi \exp\left(-2\pi i \rho r \cos(\theta)\right) \\ &\qquad \left(P(\rho) - 1\right) \omega \sin(\theta)^{d-2} d\theta r^{d-1} \, d\rho \end{aligned}$$

where ω is the area of unit sphere in $(d-1)$ dimension. Next, using the identity involving bessel function of order v, i.e.,

$$\begin{aligned} J_v(2\pi t) &= \frac{(2\pi t)^v}{(2\pi)^{v+1}} \int_0^\pi \exp\left(-2\pi i t \cos(\theta)\right) \\ &\qquad \omega \sin(\theta)^{2v} \, d\theta, \end{aligned}$$

we obtain

$$\begin{aligned} G(r) &= \\ 1 &+ \frac{2\pi}{N} r^{1-\frac{d}{2}} \int_0^\infty \rho^{\frac{d}{2}-1} J_{\frac{d}{2}-1}(2\pi\rho r)\rho(P(\rho)-1)\, dk. \end{aligned}$$

C Proof for Theorem 2 from the main paper

The proof follows from [23] and provided here for completeness.

Let us denote the Fourier domain without the DC peak frequency as Θ. Since homogeneous sampling patterns have statistical properties that are invariant to translation, it is equivalent to studying the error due to the translated version of each realization, with the average computed over all translations. Formally, we can treat the torus as the group of translations, so that $\tau(S)$ denotes the translation of S by an element $\tau \in \mathcal{T}^d$. Then, averaging equation (7) over all translations of S, we get:

$$\begin{aligned} \text{gen}(h) &\triangleq \frac{1}{N^2} \int_{\mathcal{T}^d \times \Theta \times \Theta} \mathbb{E}(\mathcal{F}_{\mathcal{T}(S),l}(\mathbf{k},\mathbf{k}'))d\mathbf{k}d\mathbf{k}'d\tau, \\ &= \frac{1}{N^2} \int_{\mathcal{T}^d \times \Theta \times \Theta} \mathbb{E}(\mathcal{F}_{S,l}(\mathbf{k},\mathbf{k}')) \times \\ &\qquad \exp^{i2\pi\tau\cdot(\mathbf{k}'-\mathbf{k})}\, d\mathbf{k}d\mathbf{k}'d\tau, \end{aligned} \tag{16}$$

where the exponential arises from the translation of the sample design by a vector τ in the Fourier domain. When $\mathbf{k} \neq \mathbf{k}'$, the integral of the exponential part equals zero, so that only the case $\mathbf{k} = \mathbf{k}'$ contributes to the variance. Hence, we can remove one integral over Θ and obtain

$$\text{gen}(h) \triangleq \frac{1}{N^2} \int_\Theta \mathbb{E}(\mathcal{F}_{S,l}(\mathbf{k},\mathbf{k})) \int_{\mathcal{T}^d} d\mathbf{k}d\tau \tag{17}$$

$$= \frac{1}{N^2} \int_\Theta \mathbb{E}(\|\mathcal{F}_{S,l}(\mathbf{k},\mathbf{k})\|^2)d\mathbf{k} \tag{18}$$

Finally, denoting the power spectrum of the loss by $\mathcal{P}_l$ and the power spectrum of the sample design normalized by N as $\mathcal{P}_S$, and leveraging the fact that $\|\mathcal{F}_{S,l}(\mathbf{k},\mathbf{k})\|^2 = \|\mathcal{F}_S(\mathbf{k})\|^2 \cdot \|\mathcal{F}_l(\mathbf{k})\|^2$,

$$\text{gen}(h) \triangleq \frac{1}{N} \int_\Theta \mathbb{E}(\mathcal{P}_S(\mathbf{k}))\mathcal{P}_l(\mathbf{k})d\mathbf{k} \tag{19}$$

This provides the expression for the generalization gap in terms of the power spectra of both the sampling pattern and the loss function in the toroidal domain.

D Proof of Lemma 2 from the main paper

Note that, for a Step blue noise configuration to be realizable, it is sufficient to show that the corresponding PCF is non-negative. Thus, we have

$$\begin{aligned} & G(r) \geq 0 \\ \Leftrightarrow \quad & 1 \geq \frac{1}{N}\left(\frac{\rho_z}{r}\right)^{\frac{d}{2}} J_{\frac{d}{2}}(2\pi\rho_z r) \\ \Leftrightarrow \quad & 1 \geq \frac{1}{N}(\rho_z\sqrt{2\pi})^d \frac{J_{\frac{d}{2}}(2\pi\rho_z r)}{(2\pi\rho_z r)^{\frac{d}{2}}} \\ \Leftrightarrow \quad & 1 \geq \frac{1}{N}\frac{(\rho_z\sqrt{2\pi})^d}{2^{\frac{d}{2}}\Gamma\left(1+\frac{d}{2}\right)} \\ \Leftrightarrow \quad & \rho_z \leq \left(\frac{N\Gamma\left(1+\frac{d}{2}\right)}{\pi^{d/2}}\right)^{1/d}. \end{aligned}$$

In the last inequality, we have used the following approximation

$$J_v(x) = \frac{(x/2)^v}{\Gamma(1+v)}.$$

E Proof of Proposition 7 from the main paper

The best-case generalization gap for blue noise design is given by:

$$\text{gen}_b(h) \quad = \quad \frac{\mu(\mathcal{S}^{d-1})}{N} c_l \int_0^{\rho_0} \rho^{d-1} P_S(\rho - \rho_z^*) d\rho. \tag{20}$$

Note that, when $\rho_0 \leq \rho_z^*$ the best-case generalization error $\text{gen}_b(h) = 0$, and when $\rho_0 > \rho_z^*$, we have

$$\begin{aligned}
\text{gen}_b(h) &= \frac{\mu(\mathcal{S}^{d-1})}{N} c_l \int_{\rho_z^*}^{\rho_0} \rho^{d-1} d\rho = \frac{\mu c_l}{N} \left[\frac{\rho_0^d - \rho_z^{*d}}{d} \right] \\
&= \text{gen}_b^{\text{random}}(h) - \frac{\mu c_l \rho_z^{*d}}{Nd} \\
&= \text{gen}_b^{\text{random}}(h) - \frac{\mu c_l \Gamma\left(1 + d/2\right)}{d\pi^{d/2}}
\end{aligned} \tag{21}$$

The worst-case generalization gap can be obtained as:

$$\begin{aligned}
\text{gen}_w(h) &= \frac{\mu(\mathcal{S}^{d-1})}{N} c_l \int_0^{\rho_0} \rho^{d-1} P_S(\rho - \rho_z^*) d\rho \\
&+ \frac{\mu(\mathcal{S}^{d-1})}{N} c_l' \int_{\rho_0}^{\infty} \rho^{-2} P_S(\rho - \rho_z^*) d\rho
\end{aligned} \tag{22}$$

Note that, when $\rho_0 \leq \rho_z^*$ the worst-case generalization error $\text{gen}_w(h) = \frac{\mu c_l'}{N \rho_z^*}$, and when $\rho_0 > \rho_z^*$,

$$\begin{aligned}
\text{gen}_w(h) &= \frac{\mu(\mathcal{S}^{d-1})}{N} c_l \int_{\rho_z^*}^{\rho_0} \rho^{d-1} d\rho \\
&\quad + \frac{\mu(\mathcal{S}^{d-1})}{N} c_l' \int_{\rho_0}^{\infty} \rho^{-2} d\rho \\
&= \frac{\mu c_l}{N} \left[\frac{\rho_0^d - \rho_z^{*d}}{d} \right] + \frac{\mu c_l' \rho_0^{-1}}{N} \\
&= \text{gen}_b(h) + \frac{\mu c_l' \rho_0^{-1}}{N} \\
&= \text{gen}_w^{\text{random}}(h) - \frac{\mu c_l \Gamma\left(1 + d/2\right)}{d\pi^{d/2}}
\end{aligned} \tag{23}$$

F Proof of Proposition 10 from the main paper

For PDS design, the best-case generalization gap can be obtained as:

$$\begin{aligned}
& \text{gen}_b(h) \\
= \quad & \frac{\mu(\mathcal{S}^{d-1})}{N} c_l \int_0^{\rho_0} \rho^{d-1} P_S(\rho - r_{min}^*) d\rho \\
= \quad & \frac{\mu c_l \rho_0^d}{Nd} - \mu c_l (2\pi r_{min}^*)^{d/2} \int_0^{\rho_0} \rho^{\frac{d}{2}-1} J_{d/2}(\rho r_{min}^*) d\rho \\
= \quad & \text{gen}_b^{\text{random}}(h) - \mu c_l (2\pi r_{min}^*)^{d/2} \int_0^{\rho_0} \rho^{\frac{d}{2}-1} J_{d/2}(\rho r_{min}^*) d\rho \\
= \quad & \text{gen}_b^{\text{random}}(h) \\
& - \mu c_l (2\pi)^{d/2} r_{min}^* \int_0^{\rho_0} (\rho r_{min}^*)^{\frac{d}{2}-1} J_{d/2}(\rho r_{min}^*) d\rho
\end{aligned} \tag{24}$$

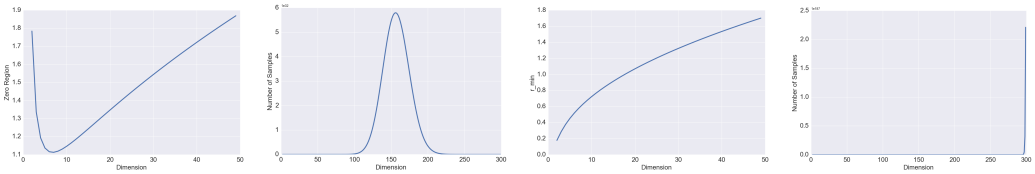

(a) (b) (c) (d)

Figure 5: (a) Maximum achievable ρ_z with $N = 10$ samples of blue noise design at varying dimensions d, (b) Minimum number of sampling points needed to achieve $\rho_z = 5$ at varying dimensions d, (c) Maximum achievable r_{min} with $N = 10$ samples of PDS at varying dimensions d, (d) Minimum number of sampling points needed to achieve $r_{min} = 1$ at varying dimensions d.

The worst-case generalization gap can be obtained as:

$$\begin{aligned}
& \text{gen}_w(h) \\
= \;& \text{gen}_b(h) + \frac{\mu(\mathcal{S}^{d-1})}{N} c_l' \int_{\rho_0}^{\infty} \rho^{-2} P_S(\rho - r_{min}^*) d\rho \\
= \;& \text{gen}_b(h) + \frac{\mu}{N} c_l' \int_{\rho_0}^{\infty} \rho^{-2} d\rho \\
& - \mu c_l' (2\pi r_{min}^*)^{d/2} \int_{\rho_0}^{\infty} \rho^{-\frac{d}{2}-2} J_{d/2}(\rho r_{min}^*) d\rho \\
= \;& \text{gen}_b(h) + \frac{\mu c_l' \rho_0^{-1}}{N} \\
& - \mu c_l' (2\pi r_{min}^*)^{d/2} \int_{\rho_0}^{\infty} \rho^{-\frac{d}{2}-2} J_{d/2}(\rho r_{min}^*) d\rho \\
= \;& \text{gen}_b(h) + \frac{\mu c_l' \rho_0^{-1}}{N} \\
- \;& \mu c_l' (2\pi)^{\frac{d}{2}} r_{min}^{*d+2} \int_{\rho_0}^{\infty} (\rho r_{min}^*)^{-\frac{d}{2}-2} J_{\frac{d}{2}}(\rho r_{min}^*) d\rho
\end{aligned} \tag{25}$$

G Generalization Gap Bounds for Poisson Disk Sample Design

Best Case

$$\begin{aligned}
\text{gen}_b(h) &= \text{gen}_b^{\text{random}}(h) \\
&\quad - \mu c_l (2\pi)^{d/2} r_{min}^* \int_0^{\rho_0} (\rho r_{min}^*)^{\frac{d}{2}-1} J_{\frac{d}{2}}(\rho r_{min}^*) d\rho \qquad (26) \\
&= \text{gen}_b^{\text{random}}(h) \\
&\quad - \mu c_l (2\pi)^{d/2} \int_0^{r_{min}^* \rho_0} \rho^{\frac{d}{2}-1} J_{d/2}(\rho) d\rho \qquad (27) \\
&\leq \text{gen}_b^{\text{random}}(h) \\
&\quad - \frac{\mu c_l (2\pi)^{d/2} 2^{\frac{-d}{2}} (\rho r_{min}^*)^d}{d\Gamma(1+\frac{d}{2})} \left(1 - \frac{1}{8} \frac{d(\rho r_{min}^*)^2}{(1+\frac{d}{2})^2}\right) \qquad (28) \\
&= \frac{\mu c_l \Gamma^{\frac{2}{d}} (1+\frac{d}{2}) \rho_0^{2+d}}{8\pi (1+\frac{d}{2})^2} \frac{1}{N^{1+\frac{2}{d}}} \qquad (29)
\end{aligned}$$

The second inequality above is based on the series form of the hypergeometric function and the assumption that N is a large number.

H Convergence Analysis of Generalization Gap with Dimensions

In this section, we report some interesting observations when analyzing the generalization gap with increasing dimensions.

H.1 Analysis with Traditional Metrics

We study the limiting behavior of ρ_z^* and r_{min}^* as d approaches infinity. We show that the analysis with conventional metrics to characterize the zero region, i.e., the range of frequencies that can be represented with no aliasing, provides some rather counter-intuitive results.

Proposition 11. *As the dimension d approaches infinity, the maximum achievable zero region for blue noise design, with a fixed N, goes to infinity, i.e., $\lim_{d\to\infty} \rho_z^* = \infty$ and, the minimum number of samples needed to achieve a zero region ρ_z approaches zero, i.e., $\lim_{d\to\infty} N = 0$.*

Intuitively, with growing d, one might expect $\rho_z^* \to 0$ and $N \to \infty$. To better understand this result, we study the relationship between these two quantities and the volume of a hyper-sphere. One of the surprising facts about a sphere in high dimensions is that as the dimension increases, the volume of the sphere goes to zero which justifies the above results. Our intuitions about space are formed in two or three dimensions and often do not hold in high dimensions. A more surprising fact is that ρ_z^* and N are not monotonic functions with respect to d (see Figure 5(a) and 5(b)). Either a steady increase or a steady decrease seems more plausible than having these two quantities grow for a while, then reach a peak at some finite value of d, and thereafter decline. This behavior has also been observed in high dimensional geometry while analyzing the volume of a hypersphere, however, no physical interpretation or intuition currently exists for this open research problem [12].

Similarly, we study the asymptotic behavior of the maximum achievable r_{min} for a fixed sample budget, and equivalently the minimum number of samples required to achieve a PDS with a given r_{min}, as the dimension grows to infinity.

Proposition 12. *As the dimension d approaches infinity, the maximum achievable r_{min} for PDS design, with a fixed number of samples, goes to infinity, i.e., $\lim_{d\to\infty} r_{min}^* = \infty$ and, the minimum number of samples needed to achieve a r_{min} also approaches infinity, i.e., $\lim_{d\to\infty} N = \infty$.*

The results in the proposition above are reasonable, since the space is growing exponentially fast.

H.2 New Metrics for Reliable Analysis

Analysis with the metric ρ_z^* which are based on the amplitude of the frequency vector, i.e., $\mathbf{k}$, to characterize the zero region, leads to inconsistent results in high dimensions. We argue that comparing ρ_z^* and r_{min}^* across different dimensions is not accurate, and these inconsistent results are a byproduct of the improper comparisons. Note that, each d-dimensional space is comprised of a different range of frequency components, and comparing the magnitude of the frequency vector directly across dimensions is questionable. In particular, for a valid comparison of volumes across dimensions, we propose to measure them in terms of a standard volume in that dimension, i.e., unit hypercube or the measure polytope, which has a volume of 1 in all dimensions. Further, as the dimension d increases, the maximum possible distance between two points in a hypercube grows as $\sqrt{d}$. Consequently, to have the same scale across dimensions, we normalize the radius of the hypersphere by a factor $\sqrt{d}$. In summary, we introduce the *relative zero region*, i.e., $\hat{\rho}_z^* = \rho_z^*/\sqrt{d}$ ($\hat{r}_{min}^* = r_{min}^*/\sqrt{d}$) for meaningful convergence analysis across dimensions.

Proposition 13. *As dimension d approaches infinity, the maximum achievable relative ρ_z^* converges to a constant, i.e.,*

$$\lim_{d\to\infty} \hat{\rho}_z^* = \frac{1}{\sqrt{2\pi e}},$$

and the minimum number of blue noise samples needed to achieve $\hat{\rho}_z^*$ goes to infinity.

Proof. To prove the first identity, note that $\frac{\rho_z^*}{\sqrt{d}} = \frac{\sqrt[d]{N}}{\sqrt{\pi d}} \sqrt[d]{\Gamma\left(1+\frac{d}{2}\right)}$ and invoke Stirling's approximation, i.e., $\Gamma(1+m) = \left(\frac{m}{e}\right)^m \sqrt{2\pi m}$. Now, the required result can be obtained by letting d approach infinity. The second identity can be proved in a similar manner. □

Similarly, we study the asymptotic behavior of $\hat{r}^*_{min}$ for PDS sampling.

Proposition 14. *As dimension d approaches infinity, the maximum achievable relative r^*_{min} converges to a constant, i.e.,*

$$\lim_{d\to\infty} \hat{r}^*_{min} = \frac{1}{\sqrt{2\pi e}}$$

and, the minimum number of PDS samples needed to achieve $\hat{r}^*_{min}$ goes to infinity.

Proof. Proof is similar to the one as in Proposition equation 13 and, thus, omitted. □

The results in Propositions 13 and 14 show interesting limiting behaviors of both blue noise and PDS designs.

References

[1] Zeyuan Allen-Zhu, Yuanzhi Li, Aarti Singh, and Yining Wang. Near-optimal design of experiments via regret minimization. In *Proceedings of the 34th International Conference on Machine Learning-Volume 70*, pages 126–135. JMLR. org, 2017.

[2] Rushil Anirudh, Jayaraman J Thiagarajan, Peer-Timo Bremer, and Brian K Spears. Improved surrogates in inertial confinement fusion with manifold and cycle consistencies. *Proceedings of the National Academy of Sciences*, 117(18):9741–9746, 2020.

[3] R Betti and OA Hurricane. Inertial-confinement fusion with lasers. *Nature Physics*, 12(5):435, 2016.

[4] Stéphane Boucheron, Olivier Bousquet, and Gábor Lugosi. Theory of classification: A survey of some recent advances. *ESAIM: probability and statistics*, 9:323–375, 2005.

[5] Olivier Bousquet and André Elisseeff. Stability and generalization. *Journal of machine learning research*, 2(Mar):499–526, 2002.

[6] Luca Brandolini, Leonardo Colzani, and Andrea Torlaschi. Mean square decay of fourier transforms in euclidean and non euclidean spaces. *Tohoku Mathematical Journal, Second Series*, 53(3):467–478, 2001.

[7] Russel E. Caflisch. Monte carlo and quasi-monte carlo methods. *Acta Numerica*, 7:1–49, 1998.

[8] Yash Deshpande and Andrea Montanari. Linear bandits in high dimension and recommendation systems. In *2012 50th Annual Allerton Conference on Communication, Control, and Computing (Allerton)*, pages 1750–1754. IEEE, 2012.

[9] Yash Deshpande and Andrea Montanari. Linear bandits in high dimension and recommendation systems. In *2012 50th Annual Allerton Conference on Communication, Control, and Computing (Allerton)*, pages 1750–1754. IEEE, 2012.

[10] Fredo Durand. A frequency analysis of monte-carlo and other numerical integration schemes. 2011.

[11] Sushant S. Garud, Iftekhar A. Karimi, and Markus Kraft. Design of computer experiments: A review. *Computers and Chemical Engineering*, 106(Supplement C):71 – 95, 2017. ESCAPE-26.

[12] Brian Hayes. An adventure in the nth dimension. *AmericanScientist.*, 99(6):442–446, 2011.

[13] Daniel Heck, Thomas Schlömer, and Oliver Deussen. Blue noise sampling with controlled aliasing. *ACM Trans. Graph.*, 32(3):25:1–25:12, July 2013.

[14] Ralf Herbrich and Robert C Williamson. Algorithmic luckiness. *Journal of Machine Learning Research*, 3(Sep):175–212, 2002.

[15] V Roshan Joseph. Space-filling designs for computer experiments: A review. *Quality Engineering*, 28(1):28–35, 2016.

[16] B. Kailkhura, J. J. Thiagarajan, P. T. Bremer, and P. K. Varshney. Theoretical guarantees for poisson disk sampling using pair correlation function. pages 2589–2593, March 2016.

[17] Bhavya Kailkhura, Jayaraman J. Thiagarajan, Peer-Timo Bremer, and Pramod K. Varshney. Stair blue noise sampling. *ACM Trans. Graph.*, 35(6):248:1–248:10, November 2016.

[18] Bhavya Kailkhura, Jayaraman J Thiagarajan, Charvi Rastogi, Pramod K Varshney, and Peer-Timo Bremer. A spectral approach for the design of experiments: Design, analysis and algorithms. *The Journal of Machine Learning Research*, 19(1):1214–1259, 2018.

[19] Vladimir Koltchinskii and Dmitriy Panchenko. Rademacher processes and bounding the risk of function learning. In *High dimensional probability II*, pages 443–457. Springer, 2000.

[20] Alex Kulesza and Ben Taskar. Determinantal point processes for machine learning. *arXiv preprint arXiv:1207.6083*, 2012.

[21] Gowtham Muniraju, Bhavya Kailkhura, Jayaraman J Thiagarajan, Peer-Timo Bremer, Cihan Tepedelenlioglu, and Andreas Spanias. Coverage-based designs improve sample mining and hyper-parameter optimization. *arXiv preprint arXiv:1809.01712*, 2018.

[22] Art B Owen. Monte carlo and quasi-monte carlo for statistics. *Monte Carlo and Quasi-Monte Carlo Methods 2008*, pages 3–18, 2009.

[23] Adrien Pilleboue, Gurprit Singh, David Coeurjolly, Michael Kazhdan, and Victor Ostromoukhov. Variance analysis for monte carlo integration. *ACM Transactions on Graphics (TOG)*, 34(4):124, 2015.

[24] Thomas Schlömer, Daniel Heck, and Oliver Deussen. Farthest-point optimized point sets with maximized minimum distance. pages 135–142, 2011.

[25] Burr Settles. Active learning literature survey. Technical report, University of Wisconsin-Madison Department of Computer Sciences, 2009.

[26] Kartic Subr and Jan Kautz. Fourier analysis of stochastic sampling strategies for assessing bias and variance in integration. *ACM Trans. Graph*, 32:4, 2013.

[27] Huan Xu and Shie Mannor. Robustness and generalization. *Machine learning*, 86(3):391–423, 2012.